

# Analysis of a Lunar Base Structure Using the Discrete-Element Method

Axel R. Tóth<sup>1</sup> and Katalin Bagi<sup>2</sup>

**Abstract:** A lunar base structure must provide protection against various hazards such as bombardment by meteorites, radiation, or extreme changes in temperature. A possible structural solution was proposed in the literature. The lunar base, planned to be built in a long, narrow valley with solid rock walls, would consist of three main elements: a masonry vault, supported by the rock walls of the valley; a regolith layer a few meters thick on top of it to dissipate radiation and the kinetic energy of impacting meteorites, and to balance temperature; and inflatable units under the arch to serve as a living area for humans. The objective was to check the feasibility of this idea from a structural mechanics point of view. A two-dimensional discrete-element model of the vault-regolith system was constructed, and the behavior of the structure under its own weight was analyzed. Initial simulations on the effect of meteorite impacts were conducted, but a significantly improved model would be required to continue this analysis. This note summarizes the results to date. DOI: [10.1061/\(ASCE\)AS.1943-5525.0000073](https://doi.org/10.1061/(ASCE)AS.1943-5525.0000073). © 2011 American Society of Civil Engineers.

**CE Database subject headings:** Discrete elements; Masonry; Arches; Granular media; Moon; Space structures.

**Author keywords:** UDEC; Distinct element; Masonry arch; Granular material; Regolith.

## Introduction

Designers of lunar habitats have to face extreme challenges (e.g., Benaroya et al. 2008), the most important of which include the following:

- The surface temperature of the moon varies between approximately +120°C and −150°C;
- As the moon lacks an atmosphere, frequent and strong micro-meteorite bombardment endangers human life (meteorites and micrometeorites arrive to the surface with approximately a 10–30 km/s velocity); and
- According to Silberberg et al. (1985), even when levels of solar activity and cosmic radiation are low, the annual dose that humans on the surface are exposed to is about 6–10 times more than permissible, and the intensity is particularly high during periods of solar flares.

A lunar habitat should provide efficient protection against these hazards. A possible structural solution was proposed by Boldoghy et al. (2006, 2007). The lunar base, planned to be built in a long, narrow valley with solid rock walls, would consist of three main elements (see Fig. 1):

1. A masonry vault, perhaps made of cast lunar regolith, supported by the walls of the valley.

2. A thick covering layer of regolith on the vault to provide protection against primary radiation [a thickness of at least 2.5–3 m is required, according to Silberberg et al. (1985)]; and to reduce the extreme changes in temperature [a thickness of 10–15 m was proposed in Boldoghy et al. (2006)]. The regolith may also be packed into bags first, and then the covering layer can simply be formed by laying the bags on top of each other (Boldoghy et al. 2007).
3. Under the arch, in the protected area (structurally independently of the vault-regolith system), pillow-shaped inflatable units serve as living areas for humans. (Being independent of the arch, their airtightness is not endangered, even if a very high energy meteorite impact causes small slips or displacements of one or more of the blocks in the arch.)

The main mechanical advantage of the proposed solution over other proposals is that each part of the system is exposed mainly to the kind of load it is best able to resist. The regolith cover efficiently dissipates the kinetic energy of meteorite impacts; the masonry vault is under high internal compression caused by the weight of the regolith layer; the inflatable structures only have to resist the tension caused by the internal air pressure. This division of the various different mechanical tasks reduces the complexity of the internal force systems, which consequently makes the structural behavior more safe.

This work has been focusing on the numerical analysis of the feasibility of this idea. A cross section of the masonry vault and of the regolith layer (see Fig. 1) was simulated with the help of UDEC, a two-dimensional (2D) discrete-element code (Cundall 1971; Itasca Consulting Group 2005). (Since the inflatable units are independent of the arch-regolith system in this concept, this study did not deal with the inflatables in this analysis.) Designs with different geometrical arrangements and dimensions were modeled. The process of depositing the regolith layer was simulated with UDEC for the different arrangements, and the stability of the masonry arch was monitored throughout the process. Initial simulations of the effect of meteorite impacts were conducted.

<sup>1</sup>Hungarian State Railways (M'V Zrt.), H-1087 Budapest, Kerepesi út 3., Hungary. E-mail: axeltoth@yahoo.co.uk

<sup>2</sup>Dept. of Structural Mechanics, Budapest Univ. of Technology and Economics, H-1521 Budapest, Műegyetem rkp. 3. K.mf. 35., Hungary (corresponding author). E-mail: kbagi@mail.bme.hu

Note. This manuscript was submitted on February 28, 2010; approved on July 29, 2010; published online on August 13, 2010. Discussion period open until December 1, 2011; separate discussions must be submitted for individual papers. This technical note is part of the *Journal of Aerospace Engineering*, Vol. 24, No. 3, July 1, 2011. ©ASCE, ISSN 0893-1321/2011/3-397–401/\$25.00.

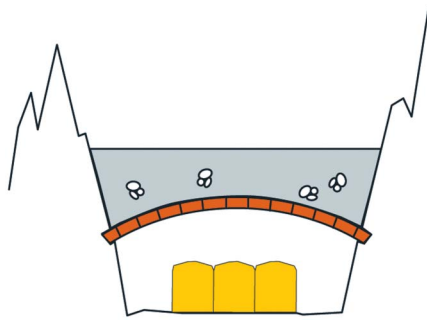


Fig. 1. Structural concept

## Numerical Model

### General Overview of the Simulation Technique

A discrete-element model considers the structure to be a collection of separate blocks (discrete elements), each of which is able to move and—in most software—to deform independently of each other. The blocks may come into contact with each other, where forces can be transmitted from one block to another, causing stresses and deformations in them. There are several techniques for calculating the motions of the elements caused by the forces (external loads and contact forces) acting on them.

The code used in this study was the 2D version of UDEC (Cundall 1971; Itasca Consulting Group 2005). This code was originally developed for the simulation of fractured rocks, and today it is widely used in engineering practice and also for modeling masonry structures. The blocks are made deformable in such a way that they are divided into simplexes (triangles in 2D) that serve as uniform-strain finite elements (see Fig. 2). The nodes of these simplexes (gridpoints) are the basic units of the analysis. The mass of a gridpoint is defined with the help of the volume (area in 2D) of the Voronoi cell around that gridpoint within the element, and different forces (e.g., weight, distributed forces expressed by neighboring Voronoi-cells because of the stresses inside the simplexes, and contact forces transmitted from contacting elements) may act on this volume assigned to the gridpoint. The displacements of these nodes during a small finite  $\Delta t$  time interval are calculated by Newton's second law of motion. An explicit time-integration scheme, based on central differences, is used for following the mechanical behavior (motions, changes of forces, and stresses) over time: the simulation of the state change is achieved by step-by-step calculation of the motions of the gridpoints.

### Model of the Arch-Regolith System

Fig. 3 shows the three main components of the model, which are detailed in the following.

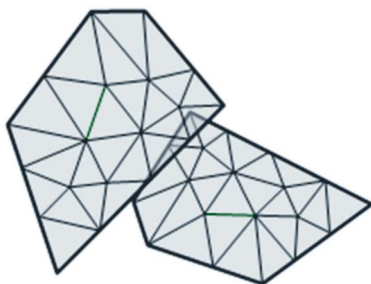


Fig. 2. Discrete elements in UDEC: subdivision into triangles

### Masonry Vault

The analyzed 2D slice of the vault consisted of 19 blocks (their indexes are also shown in Fig. 3), the left and right edges of which were embedded into the rock wall. The span of the arch was 10 m. The material, i.e., cast regolith, was modeled as a linearly elastic, isotropic continuum. According to Ruess et al. (2006), the Young's modulus was  $E = 100$  GPa. For the Poisson's coefficient, two different values,  $\mu = 0.2$  and  $\mu = 0.1$  were tried, but the differences in the results were negligible, so in most tests,  $\mu = 0.2$  was used. The density was  $\rho = 3,000$  kg/m<sup>3</sup>.

The  $v$  width of the arch was a variable in the tests (a typical value,  $v = 20$  cm, is shown in Fig. 3).

### Intact Rock of the Valley

The material was also modeled as a linear elastic, isotropic continuum, and the parameters were the same as those of the cast regolith:  $E = 100$  GPa,  $\mu = 0.2$ , and  $\rho = 3,000$  kg/m<sup>3</sup>. The grid points at the outer and bottom boundaries were fixed against translations, as shown in Fig. 3. The  $\beta$  slope of the valley was a variable in the simulations (a typical value was  $\beta = 80^\circ$ ).

### Regolith Backfill

In this model, the regolith cover was deposited in four layers, the first of which reaches the top of the arch, and 1 m thick for each of the remaining layers (see Fig. 3). Two different methods of upfilling the backfill were simulated.

Method (a): one layer was placed on the left half of the arch; then one layer on the right half; then a next layer on the left half again and so on (see Fig. 4, left side).

Method (b): all four layers forming the left half of the backfill were placed step by step, before starting to build the right half (Fig. 4, right side).

In both methods, a second and a third alternative to the simplest possibility of modeling the backfill as a single continuous domain were also tried. As shown in Fig. 4, the backfill could also be considered as a set of contiguous Voronoi-cells (but still a continuum inside the cells); or as a collection of separate bags ( $20 \times 70$  cm each), filled with regolith. (The simulations showed, however, that the arch behavior was insensitive to which alternative was used.)

The regolith material properties applied in the model were partly taken from literature reporting laboratory measurement results, e.g., Happel (1993), Wilkinson and DeGennaro (2007), Ruess et al. (2006), and partly estimated from terrestrial experiences. The regolith was modeled as a linear elastic, isotropic continuum with a Mohr-Coulomb plastic criterion, with an internal frictional angle of  $\phi = 40^\circ$  and a cohesion of  $c = 200$  Pa. The density of the layers was 1,000, 1,300, 1,600, and 1,900 kg/m<sup>3</sup>, depending on how many layers were placed on the top of the actual layer (being compressed by the weight of more layers indicates a higher density of the actual layer). The bulk modulus varied between 0.84–1.06 MPa (higher density indicates higher bulk modulus), and the Poisson's coefficient was  $\mu = 0.3$  in every layer (these values correspond to a Young's modulus of 1.0–1.27 MPa). These values of the material characteristics were found from a verification test: with these values, the 1,000 kN/m<sup>2</sup>/m compressional stiffness, reported by Chua et al. (1990), was matched with a 3-m-thick regolith layer in the current test.

The contacts between the blocks were frictional, with no resistance to tension. The normal and shear stiffness in the block-block contacts was  $k_n = 2.00 \cdot 10^9$  and  $k_s = 1.60 \cdot 10^9$  kN/m<sup>2</sup>/m respectively, with a frictional angle of  $\phi = 35^\circ$ . These properties for the block-regolith and regolith-regolith contacts were  $k_n = 1.00 \cdot 10^9$  kN/m<sup>2</sup>/m,  $k_s = 0.50 \cdot 10^9$  kN/m<sup>2</sup>/m,  $\phi = 20^\circ$ . These values were calculated following the advice of the UDEC manual (Itasca Consulting Group 2005).

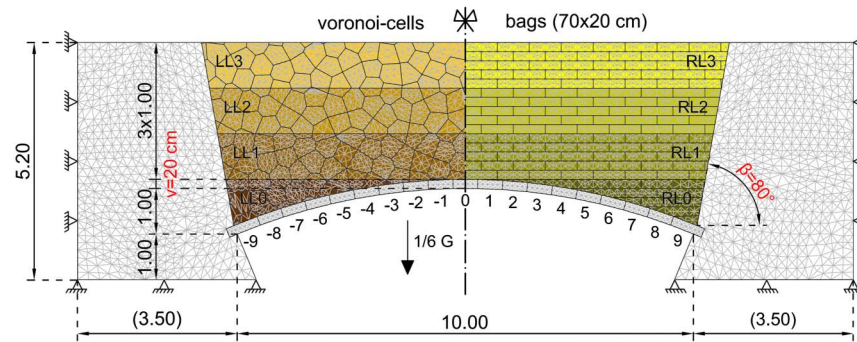


**Fig. 3.** Reference geometry: (left) regolith cover as a bulk material, modeled as a collection of contiguous Voronoi-cells; (right) regolith cover consisting of regolith filled bags

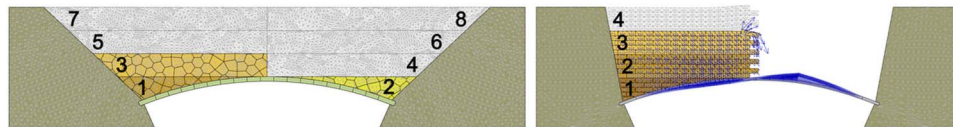


**Fig. 4.** Deposition methods and regolith models: (left) Method (a), regolith as a collection of Voronoi-cells; (right) Method (b), regolith-filled bags

The behavior of an explicit time-integration model like UDEC may strongly be influenced by the properties of the applied damping. The modeling a stone masonry arch bridge from previous experience (Tóth et al. 2009) was attributed to this study. Thus, in the simulation of the backfill deposition, a velocity-proportional damping called adaptive global damping was used, with a 50% damping dissipation ratio: viscous damping forces were used, and the viscosity constant was continuously adjusted in such a way that the power absorbed by damping was equal to 50% of the rate of change of kinetic energy in the system. The adjustment to the viscosity constant was made by a numerical servomechanism [more detailed explanations can be found in Cundall (1982) or in Itasca Consulting Group (2005)]. The length of the time step was automatically calculated by the code for every step. In the impact analysis contact damping was also activated, with  $b = 1.0$  for normal as well as for tangential directions [for the explanations on these parameters see Cundall (1982) or Itasca Consulting Group (2005) again].

The simulations were performed in two-dimensional plane strain state, with loads acting in the plane of the analysis; therefore, the width of the structure was considered to be equal to 1 m. The gravitational acceleration was 1.62 m/s, i.e., 1/6 of that on Earth. As already illustrated by Fig. 4, the simulations were done in several load steps, with each load step corresponding to depositing a new amount of regolith. After placing a new regolith mass, equilibrating cycles were repeated until the model reached the equilibrium state (defined as a state where the ratio of the average unbalanced force magnitude to the applied force magnitude does not exceed a given ratio at any gridpoint in the model), and the next step could only be followed after such a state was reached. Fig. 5 introduces the displacements of two characteristic points of the arch during such a loading process with a  $10^{-6}$  ratio. Deposition Method (a) (see Fig. 4, left side) was applied on a model with reference geometry seen in Fig. 3 (the regolith backfill is modeled as a continuum). In Fig. 5, the horizontal axis shows the number of time steps (i.e., calculation cycles). The vertical axis measures the vertical displacement of the center of Block No. -5 (solid line) and of Block Nr. 0 (broken line). Long plateaus can be seen at the end of every load step, expressing that an equilibrium

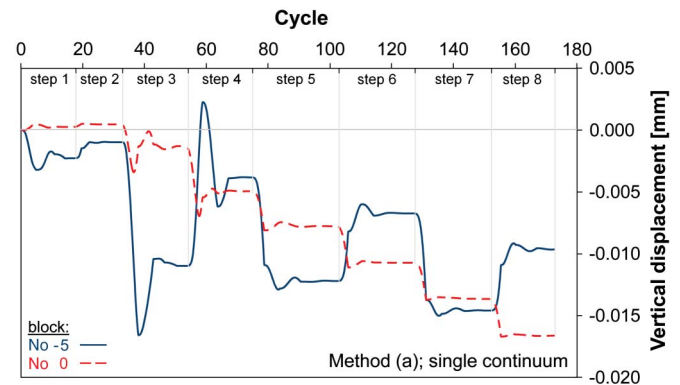


**Fig. 5.** Vertical displacements of blocks -5 and 0 during a complete loading process, Method (a), regolith model: single continuum

state was always found before placing the next amount on the already deposited layers.

## Simulations and Their Results

### Effect of Regolith Backfill Model Type

The preparation process of the backfill was simulated, following Method (a) as well as Method (b) and trying all the three backfill model types (continuum; Voronoi-cells, and bags) with and also without plastic criteria in all cases. Comparing the results of the different simulations, it was found that the backfill model type made no detectable effect on the displacements of the arch.

We also found with some surprise that the arch behavior was insensitive to whether any plastic criteria were used to model the backfill, or it was purely elastic. Figs. 6(a) and 6(b) illustrate a possible explanation. These figures show those zones of the backfill which became plastic during the actual load step [Method (a), Steps 7 and 8]. Plasticity occurred as a local phenomenon only, mainly around those small areas where the edge of a regolith domain was not supported laterally. Because the same results were



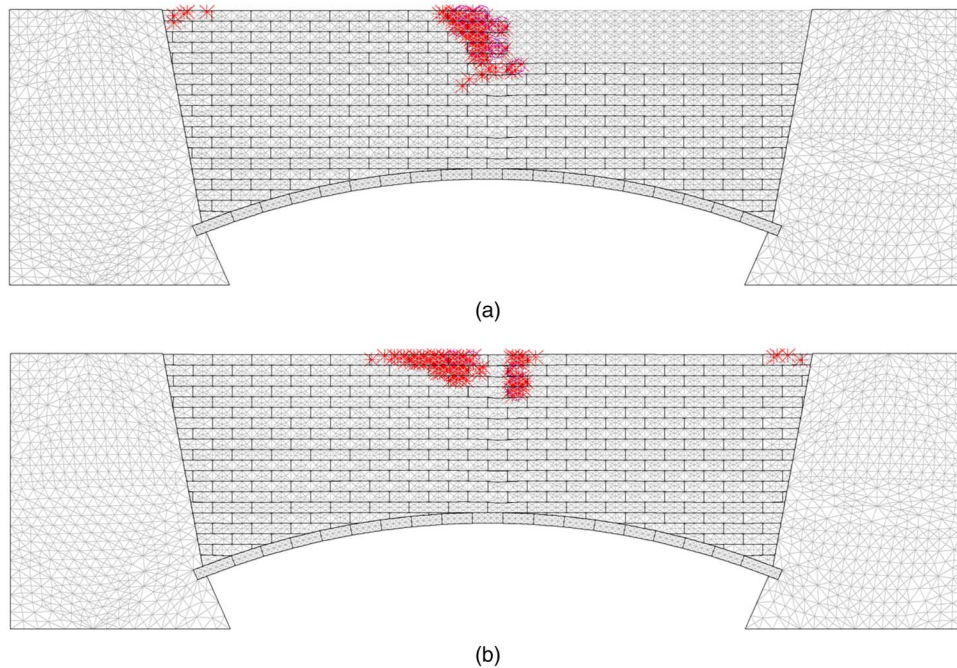


**Fig. 6.** Plastic zones in the backfill: (a) after Step 7; (b) after Step 8

found in every test, it was concluded that if the behavior of the arch is in the focus of the analysis, an elastic model would be sufficient for the backfill. Keeping in mind that an elastoplastic analysis is significantly more time-consuming than a purely elastic analysis, the rest of the tests were done with elastic models. A plastic criterion was unnecessary for the reliable description of the masonry blocks. Considering all the simulations run, the highest tensional and compressive stresses were of the order  $10^5$  N/m<sup>2</sup> and  $10^6$  N/m<sup>2</sup>, respectively, and the tensile and compressive strength of cast regolith is estimated to be  $34.5 \cdot 10^6$  N/m<sup>2</sup> and  $538 \cdot 10^6$  N/m<sup>2</sup> by Ruess et al. 2006.

### Stability of the Arch under the Weight of the Regolith Cover

Deflections of the centers of the masonry blocks for Method (a) (see Fig. 4, left side) after Step 7 and Step 8 are shown for different arch thicknesses in Fig. 7 with a wall slope of  $\beta = 80^\circ$ . The arch hardly moved, and it remained stable for all thicknesses that were tried (by stability, an equilibrium state was numerically found without the collapse of the arch).

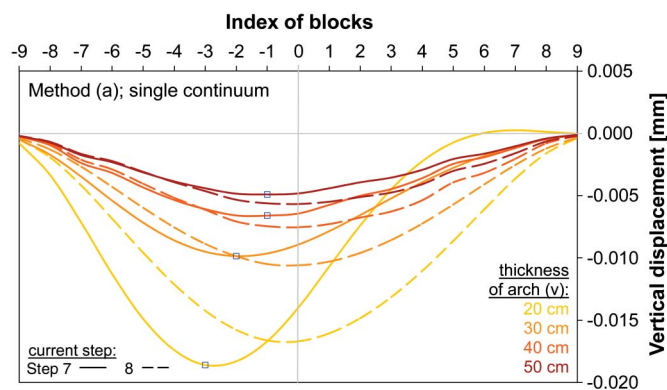


**Fig. 7.** Arch deflections in case of Method (a), regolith model: single continuum

With deposition Method (b) (see Fig. 4, right side), the arch was more sensitive to the increasing loads. There was an interest in how the arch thickness influenced the load-bearing capacity of the arch in this case. Fig. 8 shows the minimally necessary arch thicknesses that were still able to equilibrate a certain number of layers on the left half of the arch. The horizontal axis shows the number of deposited layers, and the vertical axis shows the smallest arch thickness that could still ensure the stability of the arch. (Round centimeters were considered only, so the upward right point of the diagram, for instance, represents that if carrying four layers on its left half, a 22-cm-thick arch equilibrated the weight of the upfill, but a 21-cm-thick arch collapsed.)

### Effect of Wall Slope

The simulations were repeated by trying different values for the wall slope  $\beta$  from  $30^\circ$  to  $90^\circ$ . Surprisingly, only a negligible change in the internal stresses and in the deflections of the arch were detected when  $\beta$  was varied. Because of surface friction, the intact rock apparently took part in bearing the weight of the regolith backfill.

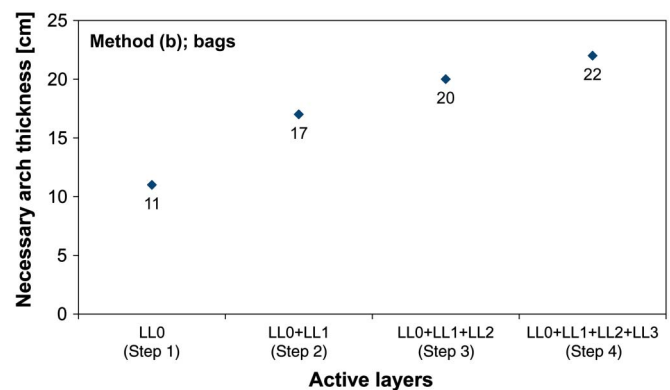


**Fig. 8.** Necessary arch thickness depending on the number of deposited layers, Method (b), regolith model: bags

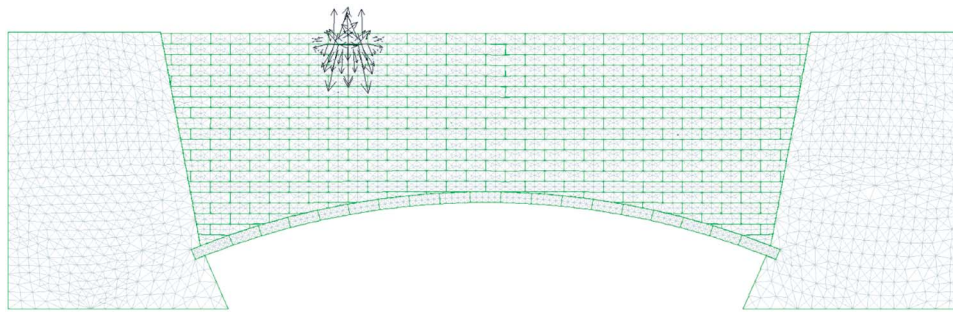


Fig. 9. Velocity vectors of the gridpoints after  $3.14 \times 10^{-3}$  s

### Ongoing Research: Dynamic Effect of Meteorite Impacts

Recently, meteorite impacts have been simulated to see how the arch behaves when meteorites hit the top of the regolith layer from different directions. At a speed of approximately 10–30 km/s, even very small micrometeorites may have a significant kinetic energy that should be dissipated by the regolith backfill to protect the masonry vault.

Up to now, the aforementioned 2D model was used in all the tests. This model is unable to follow the longitudinal effects of the pointlike impacts, so the impact results cannot directly be interpreted for three-dimensional (3D) reality. The objective with these first tests was only to gain initial experience of the dissipative and dynamic behavior of the UDEC model. To draw reliable conclusions, a 3D model is indispensable.

Bearing this in mind, different simulations of meteorite impacts were conducted. As shown in Fig. 9, a micrometeorite of  $0.14 \cdot 10^{-3}$  g hits the surface from vertical direction with a velocity of 10,000 m/s. The regolith cover consists of bags. The contact damping was also activated now with a damping coefficient  $b = 1.0$ , in addition to adaptive global damping. Because of the extremely high velocity of the impacting object, numerical problems occurred during the simulations. Within a single time step, the contact deformations between neighboring discrete elements became so large that the software could not treat them. This problem was dealt with by replacing the original mass of  $0.14 \cdot 10^{-3}$  g and velocity of 10,000 m/s of the micrometeorite by a mass of 0.14 g and velocity of 10 m/s, so that the impulse of the impacting object would be the same.

Fig. 9 shows the velocity vectors of the gridpoints in the model  $3.14 \cdot 10^{-3}$  s after the impact. The longest arrow corresponds to a 0.578 m/s velocity. The vault remained undamaged.

In addition to turning to 3D analysis, this study would need reliable physical data from laboratory measurements to calibrate the dissipative characteristics of the regolith model. So far, such data for regolith or regolith simulants have not been found in the literature. Therefore, reliable impact analysis remains a task for the future.

### Summary

We built a 2D numerical model of the structure proposed by Boldoghy et al. (2006, 2007) for lunar bases. It was found that the backfill model type (continuous, Voronoi-cells, or bags) does not affect displacements of the arch, whereas the upfilling process significantly affects the displacements of the arch. The slope of the wall has a negligible effect, but the arch thickness ( $v$ ) has a significant effect on arch displacements and on the load-bearing

capacity. A few initial tests on meteorite impacts were conducted, but because of the limitations of the model used (2D; lack of quantitative data on the dissipative behavior of regolith) they could not give reliable results. The simulation of meteorite impacts is our most important task for the future.

### Acknowledgments

The authors would like to express their gratitude to Professor Haym Benaroya for his valuable help in surveying the literature of the subject, and to Dr. T. P. Varga for the discussions that inspired this work. Our research was partly supported by the OTKA (Hungarian Research Fund) under Grant No. 48906.

### References

- Benaroya, H., and Bernold, L. (2008). "Engineering of lunar bases." *Acta Astronaut.*, 62, 277–299.
- Boldoghy, B., Kummert, J., Szilágyi, I., Varga, T., and Bérczi, Sz. (2006). "Feasibility concept of creating protected spaces with great size and balanced interior temperature for industrial activities on the moon." *Space researches roundtable VIII*, Colorado School of Mines, Boulder, CO.
- Boldoghy, B., Kummert, J., Varga, T., Szilágyi, I., and Bérczi, S. (2007). "Practical realization of covering lunar buildings for ensure levelled temperature environment." *38th Lunar and Planetary Science Conf.*, Lunar and Planetary Institute, League City, TX.
- Chua, K. M., Yuan, Z., and Johnson, S. W. (1990). "Foundation design of a large diameter radio telescope on the moon." *Proc., SPACE 90 Conf.: Engineering and Operations in Space*, ASCE, Reston, VA, 707–716.
- Cundall, P. A. (1971). "A computer model for simulating progressive large-scale movements in blocky rock systems." *Proc., Symp. of the Int. Society of Rock Mechanics*, Nancy, France, Vol. 2(8).
- Cundall, P. A. (1982). "Adaptive density-scaling for time-explicit calculations." *Proc. 4th Int. Conf. on Numerical Methods in Geomechanics*, Edmonton, Canada, 23–26.
- Happel, J. A. (1993). "Indigenous materials for lunar construction." *Appl. Mech. Rev.*, 46(6), 313–325.
- Itasca Consulting Group. (2005). *Universal distinct element code (UDEC) user's guide, Version 4.0*, Minneapolis.
- Ruess, F., Schaezlin, J., and Benaroya, H. (2006). "Structural design of a lunar habitat." *J. Aerosp. Eng.*, 19(3), 133–157.
- Silberberg, R., Tsao, C. H., Adams, J. H., and Letaw, J. R. (1985). "Radiation transport of cosmic ray nuclei in lunar material and radiation doses." *Lunar bases and space activities of the 21st century*, W. W. Mendell, ed., Lunar and Planetary Institute.
- Tóth, A. R., Orbán, Z., and Bagi, K. (2009). "Discrete element analysis of a stone masonry arch." *Mech. Res. Commun.*, 36(4), 469–480.
- Wilkinson, A., and DeGennaro, A. (2007). "Digging and pushing lunar regolith: Classical soil mechanics and the forces needed for excavation and traction." *J. Terramech.*, 44, 133–152.

Copyright of Journal of Aerospace Engineering is the property of American Society of Civil Engineers and its content may not be copied or emailed to multiple sites or posted to a listserv without the copyright holder's express written permission. However, users may print, download, or email articles for individual use.